An efficient broad-band mid-wave IR fiber optic light source: design and performance simulation

A. Barh, S. Ghosh, R. K. Varshney, and B. P. Pal*

Department of Physics, Indian Institute of Technology Delhi, New Delhi, 110016, India
*bppal@physics.iitd.ernet.in

Abstract: Design of a mid-wave IR (MWIR) broad-band fiber-based light source exploiting degenerate four-wave mixing (D-FWM) in a meter long suitably designed highly nonlinear (NL) chalcogenide microstructured optical fiber (MOF) is reported. This superior FWM bandwidth (BW) was obtained through precise tailoring of the fiber's dispersion profile so as to realize positive quartic dispersion at the pump wavelength. We consider an Erbium (Er^{3+}) - doped continuous wave (CW) ZBLAN fiber laser emitting at 2.8 μm as the pump source with an average power of 5 W. Amplification factor as high as 25 dB is achievable in the 3 – 3.9 μm spectral range with average power conversion efficiency > 32%.

OCIS codes: (060.4370) Nonlinear optics, fibers; (190.4380) Nonlinear optics, four-wave mixing; (060.4005) Microstructured fibers.

References and links

1. A. Barh, S. Ghosh, G. P. Agrawal, R. K. Varshney, I. D. Aggarwal, and B. P. Pal, "Design of an efficient mid-IR light source using chalcogenide holey fibers: a numerical study," J. Opt. **15**(3), 035205 (2013).
2. S. D. Jackson, "Towards high-power mid-infrared emission from a fibre laser," Review Articles - Nat. Photonics **6**(7), 423–431 (2012).
3. G. P. Agrawal, *Nonlinear Fiber Optics*, Academic, San Diego, Calif., (2007).
4. A. Zakery and S. R. Elliott, "Optical properties and applications of chalcogenide glasses: a review," J. Non-Cryst. Solids **330**(1-3), 1–12 (2003).
5. G. Boudebs, S. Cherukulappurath, M. Guignard, J. Troles, F. Smektala, and F. Sanchez, "Linear optical characterization of chalcogenide glasses," Opt. Commun. **230**(4-6), 331–336 (2004).
6. B. J. Eggleton, B. L. Davies, and K. Richardson, "Chalcogenide photonics," Review Articles - Nat. Photonics **5**, 141–148 (2011).
7. J. M. Harbold, F. Ö. Ilday, F. W. Wise, J. S. Sanghera, V. Q. Nguyen, L. B. Shaw, and I. D. Aggarwal, "Highly nonlinear As-S-Se glasses for all-optical switching," Opt. Lett. **27**(2), 119–121 (2002).
8. J. Hu, C. R. Menyuk, L. B. Shaw, J. S. Sanghera, and I. D. Aggarwal, "Computational study of 3-5 microm source created by using supercontinuum generation in As_2S_3 chalcogenide fibers with a pump at 2 microm," Opt. Lett. **35**(17), 2907–2909 (2010).
9. C. M. B. Cordeiro, W. J. Wadsworth, T. A. Birks, and P. S. J. Russell, "Engineering the dispersion of tapered fibers for supercontinuum generation with a 1064 nm pump laser," Opt. Lett. **30**(15), 1980–1982 (2005).
10. D. I. Yeom, E. C. Mägi, M. R. E. Lamont, M. A. F. Roelens, L. B. Fu, and B. J. Eggleton, "Low-threshold supercontinuum generation in highly nonlinear chalcogenide nanowires," Opt. Lett. **33**(7), 660–662 (2008).
11. M. R. E. Lamont, C. M. de Sterke, and B. J. Eggleton, "Dispersion engineering of highly nonlinear As_2S_3 waveguides for parametric gain and wavelength conversion," Opt. Express **15**(15), 9458–9463 (2007).
12. C. S. Brès, S. Zlatanovic, A. O. J. Wiberg, and S. Radic, "Continuous-wave four-wave mixing in cm-long chalcogenide microstructured fiber," Opt. Express **19**(26), B621–B627 (2011).
13. J. D. Harvey, R. Leonhardt, S. Coen, G. K. L. Wong, J. C. Knight, W. J. Wadsworth, and P. St .J. Russell, "Scalar modulation instability in the normal dispersion regime by use of a photonic crystal fiber," Opt. Lett. **28**(22), 2225 (2003).
14. D. W. Hewak, "The promise of chalcogenides," Nat. Photonics **5**(8), 474 (2011).
15. J. S. Sanghera, I. D. Aggarwal, L. B. Shaw, L. E. Busse, P. Thielen, V. Nguyen, P. Pureza, S. Bayya, and F. Kung, "Applications of chalcogenide glass optical fibers at NRL," J. Optoelectron. Adv. Mater. **3**, 627–640 (2001).
16. M. El-Amraoui, G. Gadret, J. C. Jules, J. Fatome, C. Fortier, F. Désévédavy, I. Skripatchev, Y. Messaddeq, J. Troles, L. Brilland, W. Gao, T. Suzuki, Y. Ohishi, and F. Smektala, "Microstructured chalcogenide optical fibers from As_2S_3 glass: towards new IR broadband sources," Opt. Express **18**(25), 26655–26665 (2010).
17. C. Lin, W. A. Reed, A. D. Pearson, and H. T. Shang, "Phase matching in the minimum-chromatic-dispersion region of single-mode fibers for stimulated four-photon mixing," Opt. Lett. **6**(10), 493–495 (1981).

#186548 - $15.00 USD Received 6 Mar 2013; revised 20 Mar 2013; accepted 21 Mar 2013; published 10 Apr 2013

18. G. Cappellini and S. Trillo, "Third-order three-wave mixing in single-mode fibers: exact solutions and spatial instability effects," J. Opt. Soc. Am. B **8**(4), 824–838 (1991).
19. C. Chaudhari, T. Suzuki, and Y. Ohishi, "Design of zero chromatic dispersion chalcogenide As_2S_3 glass nanofibers," J. Lightwave Technol. **27**(12), 2095–2099 (2009).
20. R. Sen, Central Glass and Ceramic Research Institute, Kolkata, India, Personal Communication, (2013).
21. T. Yamashita and Y. Ohishi, "Cooperative energy transfer between Tb^{3+} and Yb^{3+} ions co-doped in borosilicate glass," J. Non-Cryst. Solids **354**(17), 1883–1890 (2008).
22. G. Tao, S. Shabahang, E. H. Banaei, J. J. Kaufman, and A. F. Abouraddy, "Multimaterial preform coextrusion for robust chalcogenide optical fibers and tapers," Opt. Lett. **37**(13), 2751–2753 (2012).
23. J. S. Sanghera, C. Florea, L. Busse, B. Shaw, F. Miklos, and I. D. Aggarwal, "Reduced Fresnel losses in chalcogenide fibers by using anti-reflective surface structures on fiber end faces," Opt. Express **18**(25), 26760–26768 (2010).
24. C. Quentin, B. Laurent, H. Patrick, N. T. Nam, C. Thierry, R. Gilles, M. Achille, F. Julien, S. Frédéric, P. Thierry, O. Hervé, S. Jean-Christophe, and T. Johann, "Fabrication of low losses chalcogenide photonic crystal fibers by molding process," Proc. SPIE **7598**, 75980O, 75980O-9 (2010).
25. F. Poletti, V. Finazzi, T. M. Monro, N. G. R. Broderick, V. Tse, and D. J. Richardson, "Inverse design and fabrication tolerances of ultra-flattened dispersion holey fibers," Opt. Express **13**(10), 3728–3736 (2005).

1. Introduction

In recent years, there has been a surge and continued interest to leverage on the huge development witnessed in fiber optic telecommunication to develop fibers and fiber-based devices suitable for mid-IR spectral region (2-10 μm). Emerging potential applications like non-destructive soft tissue ablation in medical diagnostics, monitoring of combustion flow and gas dynamics through molecular absorption spectroscopy, semiconductor processing (e.g. in situ real time monitoring of plasma etch rates), and huge military applications in the mid-wave IR (MWIR) spanning 3 - 5 μm region have lately attracted a lot of research investments [1, 2]. MWIR wavelength region is particularly important since a large number of molecules undergo strong characteristic vibration band transitions in this domain, which is also known as "molecular fingerprint regime" e.g. various hydrocarbons, hydrochlorides and commonly used solvents show strong absorption in the range of 3.2 – 3.6 μm [2]. Compact fiber-based light sources for MWIR would find wide scale military applications as it is a clean atmospheric window for high power transmission leading to applications in heat sinking missiles, IR counter-measures, and also thermal imaging for low power night vision in defense. Therefore it has become strategically important to develop an efficient light source in this wavelength region.

Chalcogenide glass (S-Se-Te)-based microstructured optical fibers (MOFs) have been considered potentially very suitable for the MWIR region due to certain special properties, which could be exploited to realize devices for applications in this wavelength range [3–5]. Studies on MOFs have shown that, waveguide dispersion in them dominates over material dispersion in determining the total dispersion of such fibers. This dispersion tailoring feature along with the relatively high Kerr nonlinearity in chalcogenide glasses (achievable n_2 being as high as 100 times larger than that of conventional silica fiber) [3], in them make these fibers imminently suitable for a number of applications like signal processing [6], all optical switching [7], supercontinuum generation [8–10], wavelength translation via FWM [11–13] etc. However, realization of low transmission losses in chalcogenide MOFs is still a challenge [6]. On the other hand, their chemical durability, glass transition temperature, strength, stability etc. can be improved by doping with As, Ge, Sb, Ga for drawing an optical fiber. At present their fabrication technology is well matured though expensive [6, 14–16].

In this paper, we have numerically designed an efficient, broad-band (covering 3 - 4 μm spectral domain) mid-IR light source by exploiting the degenerate four-wave mixing (D-FWM) process through the extraordinary linear and nonlinear (NL) properties of chalcogenide glass-based MOFs by using a commercially available continuous-wave (CW) Erbium (Er^{3+}) -doped ZBLAN fiber laser emitting at 2.8 μm as a pump for the FWM process. In order to achieve broad and flat continuous spectrum around the targeted signal wavelength in the MWIR, we have designed the fiber so as to obtain low anomalous dispersion ($\beta_2 \leq 0$) and positive fourth order GVD parameter (β_4) at this pump wavelength (λ_p). Keeping these

#186548 - $15.00 USD Received 6 Mar 2013; revised 20 Mar 2013; accepted 21 Mar 2013; published 10 Apr 2013

targets in mind, a broad-band chalcogenide fiber-based efficient light source for use in the MWIR wavelength regime (3 – 3.9 μm) has been numerically designed and reported here. This work should be of interest to those involved with chalcogenide fiber fabrication for its possible fabrication, if necessary with another more suitable glass composition, and subsequent fine tuning of the design in order to realize MWIR devices.

2. Numerical modeling

In optical fibers, several nonlinear phenomena could be exploited to generate new wavelength(s). Under certain conditions, however, FWM is the dominant nonlinear mechanism for generating new wavelengths, provided a certain phase-matching condition is satisfied [3, 17]. For our design purpose we will consider input pump power (P_0) levels to be below 5 W, which is considerably lower than the threshold for the onset of stimulated Raman and Brillouin scatterings in fibers shorter than 10 m [3]. Under D-FWM process, pump photons of frequency ω_p get converted into a signal photon ($\omega_s < \omega_p$) and an idler photon ($\omega_i > \omega_p$) according to the energy conservation relation ($2\omega_p = \omega_s + \omega_i$) where, subscripts s, i and p stands for signal, idler, and pump, respectively. For efficient mixing, it is important to recognize that the following phase matching condition is satisfied:

$$\Delta\kappa = \gamma P_0 + \Delta k_L \tag{1}$$

where P_0 is the input pump power, γ is the well-known effective NL coefficient, and Δk_L is the linear phase-mismatch term that is chromatic and inter-modal dispersion dependent and is given by [3]

$$\Delta k_L = \sum_{m=2,4,6...}^{\infty} 2\beta_m(\omega_p)\frac{\Omega_S^m}{m!} + \Delta k_W \tag{2}$$

where β_m is the m^{th} order GVD parameter, Ω_s is the frequency shift ($\Omega_s = \omega_p - \omega_s = \omega_i - \omega_p$), and Δk_W is the phase mismatch term due to waveguide dispersion, which can be neglected in single-mode fibers [3]. Under CW pump condition in a highly NL fiber, the maximum Ω_s depends on both the magnitude and sign of GVD parameters. On one hand, positive β_4 leads to broad-band and flat gain where as negative β_4 reduces the flatness and BW of FWM. Thus higher order *dispersion management* is very crucial in such fiber designs. Considering up to fourth order dispersion, for positive β_4 and negative β_2, Ω_s can be approximated as

$$\Omega_s = \sqrt{\frac{6|\beta_2|}{\beta_4}\left(1 \pm \sqrt{1 - \frac{\beta_4\gamma P_0}{3\beta_2^2}}\right)} \tag{3}$$

From Eq. (3), we can see that two sets of signal and idler are generated for this particular choice of GVD and NL parameters, i.e. for two signal wavelengths (λ_s), the phase matching becomes perfect. Therefore, we have to optimize the fiber and launching parameters such that the overall signal spectrum, generated around these two phase matching λ_s become broad and flat with sufficient amplification. This positive β_4 value in the vicinity of low negative β_2 at the λ_p could be achieved by suitably adjusting the fiber parameters to optimize the waveguide dispersion and hence multi-order dispersion management is feasible to engineer the FWM efficiency.

In our design calculation, first we have studied the D-FWM performance under lossless, undepleted pump condition, where CW pump power is only transferred to signal and idler wave. The launch of a weak idler along with the pump improves the FWM efficiency since stimulated FWM is employed in place of spontaneous FWM. It may be noted that here we are referring to the idler as an input field and the new wavelength generated in the MWIR region as the signal. The peak amplification factor (*AF*) for the generated signal becomes

#186548 - $15.00 USD Received 6 Mar 2013; revised 20 Mar 2013; accepted 21 Mar 2013; published 10 Apr 2013

$$AF_S = P_{S,out}/P_{I,in} = (\gamma P_0/g)^2 \sinh^2(gL) \quad (4)$$

where $P_{S,out}$ is the peak signal power at the output, $P_{I,in}$ is the input idler power, L is the interaction length and the D-FWM amplification coefficient g is given by [3]

$$g = \sqrt{(\gamma P_0)^2 - (\Delta\kappa/2)^2} \quad (5)$$

In the next step, assuming CW conditions, we have studied the complex amplitudes A_j (z) (j = p, i, s) and powers (P_{out}) variation along fiber length to study the effect of pump depletion and material loss by numerically solving the following three coupled amplitude Eqs [18]:

$$\frac{dA_p}{dz} = -\frac{\alpha_p A_p}{2} + \frac{in_2\omega_p}{c}\left[\left(f_{pp}|A_p|^2 + 2\sum_{k=i,s} f_{pk}|A_k|^2\right)A_p + 2f_{ppis}A_p^* A_i A_s e^{j\Delta k_L z}\right] \quad (6)$$

$$\frac{dA_i}{dz} = -\frac{\alpha_i A_i}{2} + \frac{in_2\omega_i}{c}\left[\left(f_{ii}|A_i|^2 + 2\sum_{k=p,s} f_{ik}|A_k|^2\right)A_i + f_{ispp}A_s^* A_p^2 e^{-j\Delta k_L z}\right] \quad (7)$$

$$\frac{dA_s}{dz} = -\frac{\alpha_s A_s}{2} + \frac{in_2\omega_s}{c}\left[\left(f_{ss}|A_s|^2 + 2\sum_{k=p,i} f_{sk}|A_k|^2\right)A_s + f_{sipp}A_i^* A_p^2 e^{-j\Delta k_L z}\right] \quad (8)$$

where α_j is the loss at the wavelength λ_j, n_2 is the NL index coefficient and Δk_L is the linear phase mismatch defined in Eq. (2). The overlap integrals (f_{jk} and f_{ijkl}) are defined as

$$f_{jk} = \frac{\left\langle |F_j|^2 |F_k|^2 \right\rangle}{\left\langle |F_j|^2 \right\rangle \left\langle |F_k|^2 \right\rangle} \qquad f_{ijkl} = \frac{\left\langle F_i^* F_j^* F_k F_l \right\rangle}{\left[\left\langle |F_i|^2 \right\rangle \left\langle |F_j|^2 \right\rangle \left\langle |F_k|^2 \right\rangle \left\langle |F_l|^2 \right\rangle\right]^{1/2}} \quad (9)$$

where F_j (x,y) is the spatial distribution of the fiber mode in which the j^{th} field propagates inside the fiber.

3. Proposed fiber design

To achieve such tailored application-specific fiber designs, we focus on an arsenic sulphide (As_2S_3)-based MOF geometry with a solid core and holey cladding, consisting of 4 rings of hexagonally arranged holes embedded in As_2S_3 matrix. Generally, high index material like As_2S_3 shows normal dispersion (+ β_2) around our proposed pump wavelength (2.8 μm). But by proper tuning of the waveguide dispersion in a MOF structure, we can achieve desired value of β_2 along with either a negative β_4, which reduces the flatness and bandwidth of the FWM gain, or a relatively high positive β_4 at the expense of much smaller transverse dimensions, resulting in an even lower bandwidth. To tailor this 4th order GVD parameter, waveguide dispersion should outweigh the material one. This can be achieved by reducing core-cladding refractive index difference (Δn) appropriately to achieve the desired waveguide dispersion. In order to reduce Δn, we assume that borosilicate glass rod would fill the holes. Compatible thermal properties of the As_2S_3 and borosilicate glass should allow feasibility of fabrication of such a holey MOF [19]. The wavelength dependence of the linear refractive index of As_2S_3 and borosilicate glass has been incorporated through Sellmeier formula [19]. To suppress the modal loss, cutoff wavelength for 1st higher order mode need to be as low as possible (below λ_p). One way to achieve this is to maintain the ratio for hole-diameter to pitch (d/Λ) of the MOF below 0.45 as found by us during numerical simulations. However, during the numerical optimization process we observed that it is quite difficult to simultaneously achieve a negative β_2 and a positive β_4 for $d/\Lambda < 0.45$; some increase beyond this value of d/Λ is needed as a tradeoff between a pure single-mode guiding regime and a few modes guiding

#186548 - $15.00 USD Received 6 Mar 2013; revised 20 Mar 2013; accepted 21 Mar 2013; published 10 Apr 2013

regime. We have optimized our fiber design for a d/Λ of 0.5, at which though the next higher order mode can co-exist with the fundamental mode; our numerical study reveals that its confinement loss (α_c) is more than 5 orders of magnitudes higher than that of the fundamental mode over the entire spectral regime considered and hence would leak away with propagation within a very short length of the designed fiber. This would make the designed fiber an "effectively single-mode fiber". Additionally, to enhance the magnitude of γ and to minimize the α_c, A_{eff} should be as low as possible at both λ_p and λ_s. To attain sufficient signal amplification over the MWIR regime of 3 ~3.9 μm, we have assumed commercially available CW Er^{3+}-doped ZBLAN fiber laser emitting at 2.8 μm [2] as the pump and confined our numerical study to pump power levels below 5 W to suppress other potential NL effects. Dispersion parameters as well as the modal field were calculated by using commercially available CUDOS® software along with MATLAB® for solving the coupled differential Eqs. numerically. During optimization of the MOF structure, a strong interplay was observed between Ω_s, parametric amplification, and α_c with variations in d and Λ. After optimization a high amplification at the generated λ_s (up to 4 μm) was achieved for d/Λ = 0.5, Λ = 2.5 μm (shown in Fig. 1) with a significantly low α_c (0.01 to 0.001 dB/m) at the λ_p. For this structure, the mode field is confined almost inside the core region. Thus for short fiber lengths, which is indeed the case here, material loss of only As_2S_3 core region is considered in our simulation study. Additionally due to this tight confinement of light inside As_2S_3 core, the mode fields experience almost uniform nonlinearity during propagation. Wavelength dependence of dispersion coefficient (D) and GVD parameters β_2 and β_4 are shown in Figs. 2(a) and 2(b), respectively.

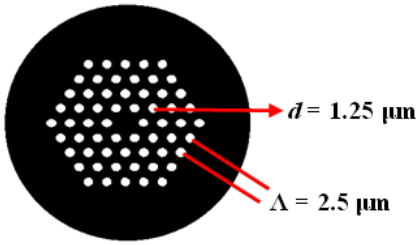

Fig. 1. Cross sectional view of the designed MOF. Cladding consists of 4 rings of borosilicate rods (white circles) embedded in the As_2S_3 matrix (black background). The diameter of the rod is d, and the centre to centre separation is denoted as pitch (Λ).

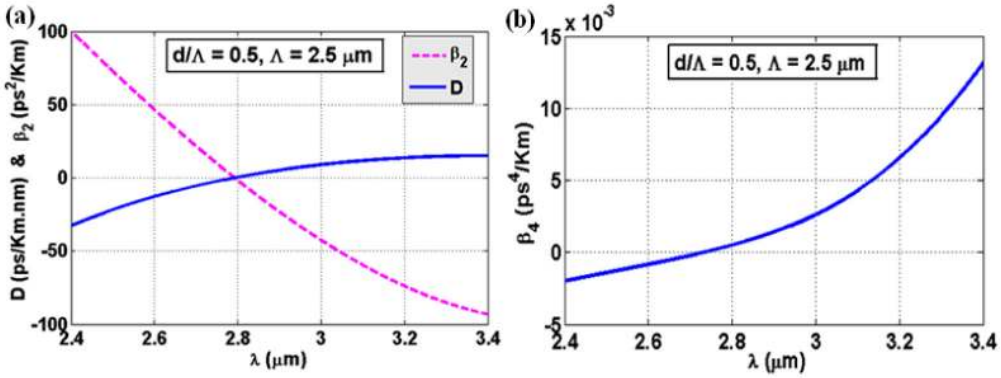

Fig. 2. Dispersion characteristics of As_2S_3 and Borosilicate based solid core MOF for d/Λ = 0.5 and Λ = 2.5 μm. (a) D (blue solid curve) and β_2 (pink dashed curve) variation with operating wavelength (λ); λ_{ZD} = 2.792 μm. (b) Variation of β_4 with λ.

#186548 - $15.00 USD Received 6 Mar 2013; revised 20 Mar 2013; accepted 21 Mar 2013; published 10 Apr 2013

Figure 2(a) clearly indicates that λ_{ZD} falls at 2.792 μm, which is slightly below the λ_p. At a fixed P_0, maximum amplification ($AF_{s,max}$) depends on γ and length of the fiber (L) as it increases exponentially with "$\gamma P_0 L$". But BW is inversely proportional to this L as long as $L >> L_{NL}$ (= $(\gamma P_0)^{-1}$). Thus to maintain large BW, L should be relatively short at the cost of peak amplification.

4. D-FWM performance under undepleted pump and lossless condition

During optimization of high-flat gain and maximum BW, a strong interplay was evident amongst P_0, L, and λ_p. If we detune λ_p from λ_{ZD}, absolute value of β_2 increases leading to fluctuations in the output spectrum due to change in $\Delta\kappa$ around its zero value. This makes the spectrum less uniform as shown in Fig. 3(a); where only upper side of λ_p is shown. In the vicinity of λ_p, the gain parameter AF_s decreases rapidly as λ_s approaches λ_p. When the phase mismatch term becomes γP_0, the AF_s becomes $(1 + \gamma P_0 L)$ leading to a linear growth of signal from λ_p. From this figure, it can be interpreted that the best result could be achieved for $\lambda_p \approx 2.797$ μm, where BW can be maximized. The GVD parameters β_2 and β_4 at this λ_p were -1.20948 ps^2/Km and 3.71480 x 10^{-4} ps^4/Km, respectively. Calculated A_{eff} at this wavelength came out to be quite small ~9.2 μm^2, which also helps in increasing the effective nonlinearity. With 2.797 μm as the pump, and fixing P_0 at 5 W, we have studied the variation of gain spectrum for different values of fiber length (shown in Fig. 3(b)). This figure clearly indicates that the maximum AF_s increases with increase in L but at the cost of narrower BW. Thus to obtain high amplification of more than 35 dB optimum set of parameter were found to be P_0 = 5W, L = 1 m, and λ_p = 2.797 μm (shown in Fig. 3(b)). The achievable full width at half maxima (FWHM) is ~670 nm with confinement loss < 0.01 dB/m across the entire BW.

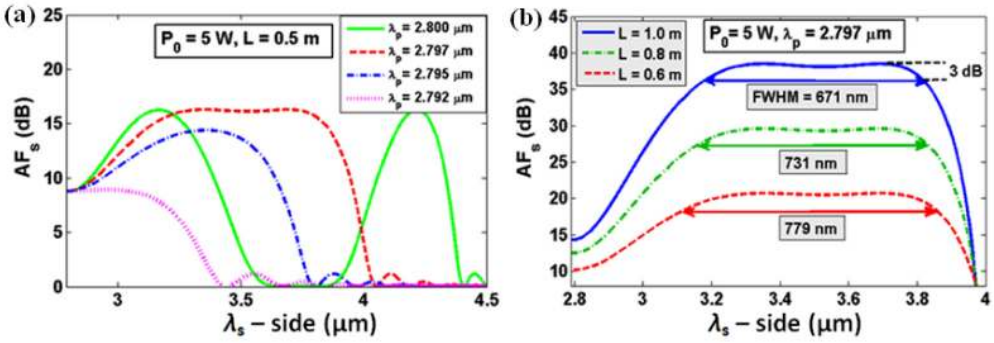

Fig. 3. (a) Variation of signal amplification factor (AF_s) for different λ_p is shown. With λ_p coinciding at λ_{ZD} (= 2.792 μm), output signal spectrum is almost uniform around λ_p. With increase in λ_p from λ_{ZD}, the BW as well as fluctuation increases. (b) Variation of AF_s for a pump power of 5 W at 2.797 μm for different L (0.6 – 1.0 m).

5. D-FWM performance under depleted pump including material loss

We now consider the material loss as reported earlier to be < 0.2 dB/m for the entire signal wavelength range [8]. We have fixed the designed fiber length (L) at 1 m, P_0 at 5 W and λ_p at 2.797 μm. The generated two signal wavelengths for which the phase matching is almost perfect were 3.12 μm and 3.85 μm, and corresponding λ_i's were 2.53 μm and 2.19 μm. Optimizing the spectral width as well as their phase matching λ_s position, broad and flat spectrum can indeed be realizable.

To study the evolution of amplitudes (A_j), output powers (P_{out}), and AF of pump, signal and idler along the propagation length (L), we numerically solved the three coupled amplitude Eqs. (6)-(8) for P_0 = 5 W, λ_p = 2.797 μm, λ_s = 3.85 μm and $P_{I,in}$ = 10 mW. Variations of A_j, P_{out} and AF are shown in Figs. 4(a)-4(c), respectively. From these figures we can see that

#186548 - $15.00 USD Received 6 Mar 2013; revised 20 Mar 2013; accepted 21 Mar 2013; published 10 Apr 2013

even considering pump depletion and material loss, more than 1 W of output signal power is achievable.

We have also optimized the $P_{I,in}$ to get maximum $P_{S,out}$ for 1 m of fiber length. These results are compiled in tabulated form in Table 1, for L = 1 m, P_0 = 5 W, λ_p = 2.797 μm and λ_s = 3.85 μm, 3.12 μm. From this table it can be easily appreciated that to get a flat and broad output spectrum at the signal side, $P_{I,in}$ should lie between 8 to 11 mW. For 10 mW of $P_{I,in}$, the average output signal power over the entire output signal band is ≈1.64 W. Thus the power transfer efficiency ($P_{S,out}/P_0$) for this case is ~32.8%, which is quite significant as a broad-band mid-IR light source. The entire output spectrum including both the idler and signal side is shown in Figs. 5(a) and 5(b), respectively, where for four different $P_{I,in}$, the variation of amplification factor is studied.

Table 1. Variation of output signal power with input idler power

$P_{I,in}$ (mW)	$P_{S,out}$ (W) (λ_s = 3.85 μm)	$P_{S,out}$ (W) (λ_s = 3.12 μm)
20	1.3611	1.4135
15	1.4277	1.6595
12	1.4505	1.7356
11	1.4523	1.7724
10	1.4496	1.8189
8	1.4248	1.8376
5	1.2959	1.8314

Though the spectral BW is almost same like undepleted (i.e. loss less case), the maximum AF_s decreases to ≈25 dB due to inclusion of pump depletion and spectral dependence of material loss. Such a fiber, if experimentally realized should be attractive as a mid-IR light source for a variety of applications outlined in the Introduction section.

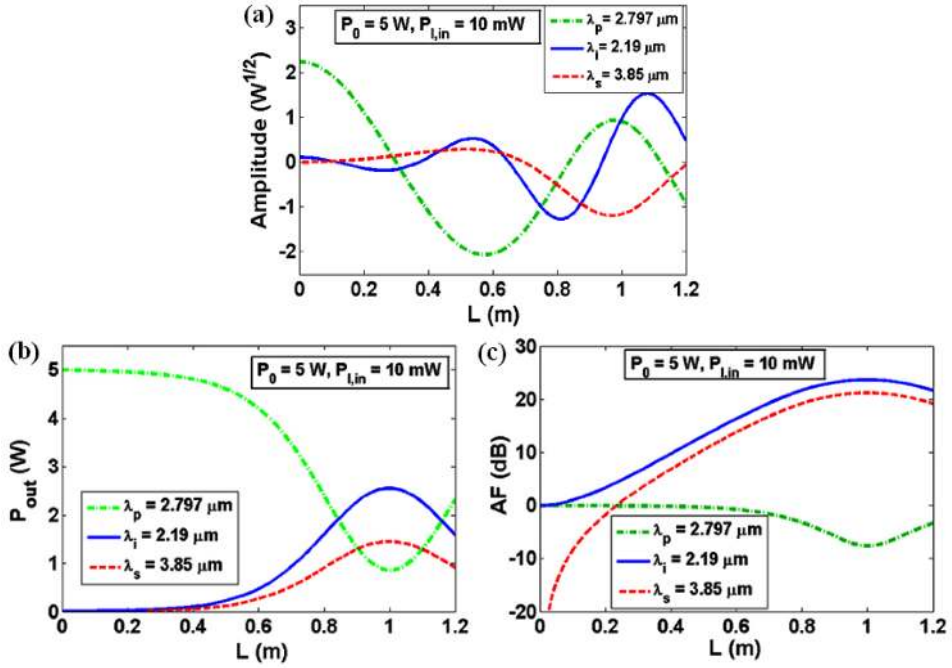

Fig. 4. Variations of (a) amplitude, (b) output power (P_{out}) and (c) amplification factor (AF) of pump, signal and idler with the fiber length (L) are shown. A weak idler of 10 mW at 2.19 μm is assumed along with 5 W of pump to initiate this D-FWM.

#186548 - $15.00 USD Received 6 Mar 2013; revised 20 Mar 2013; accepted 21 Mar 2013; published 10 Apr 2013

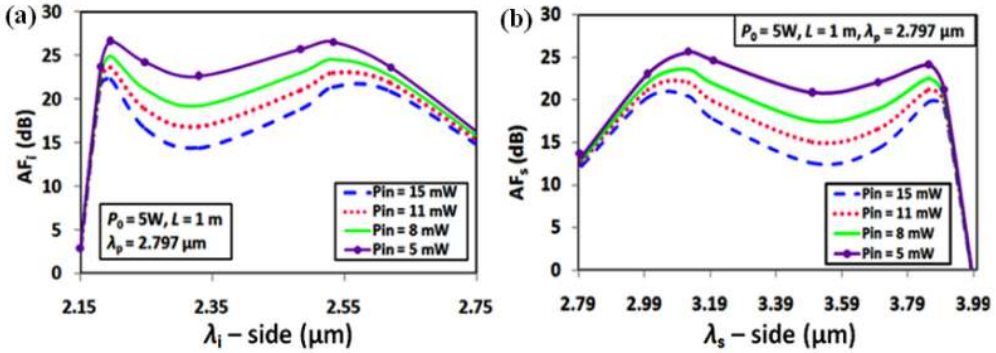

Fig. 5. Variation of amplification factor (*AF*) for different $P_{1,in}$ with pumping at 2.792 μm, L = 1 m and P_0 = 5 W. (a) The idler side of spectrum. (b) The signal side of spectrum. AF_s as high as 25 dB is achievable, where overlap between two signal spectrum (one around 3.12 μm and another around 3.85 μm) makes the entire spectrum (3 – 3.9 μm) almost uniform.

6. Conclusions and remarks

We report a theoretical design of a broad-band MWIR light source by maximizing D-FWM band-width and efficiency in a highly nonlinear chalcogenide MOF. Through a detailed numerical and analytical study, for the first time to the best of our knowledge, we have shown that MWIR power levels in excess of 1 W are achievable over the wavelength range of 3.1 – 3.9 μm with an amplification factor more than 25 dB for a 2.8 μm pump of 5W average power through a meter long specialty fiber based on our design. Additionally, a high power conversion efficiency (> 32%), and a very low confinement loss (< 0.01 dB/m) over the entire generated signal wavelength band should make our design route very attractive for making an all-fiber MWIR light source. This proposal is possibly first such proposal where a new avenue of generating significant output in the MWIR region is shown, where our contention was to theoretically prove feasibility of a new fiber design route with the potential to realize a fiber-based broad-band light source for shortwave IR region. We feel that our design route is novel and requires complex balance of design parameters to achieve desired group velocity dispersion parameters β_2 and β_4 and of appropriate signs as well as targeting zero dispersion at a wavelength commensurate to availability of high power pump lasers for achieving efficient FWM. Potential application areas could be mid-IR spectroscopy, medical diagnostics, sensing, thermal imaging, astronomy and defense since the generated wavelength matches the second low-loss transparency window of the terrestrial atmosphere and the "fingerprint regime" for large number of molecules.

It would be interesting to undertake fabrication of chalcogenide fibers based on this design, though there could be several fabrication challenges like maintaining the required d, Λ values throughout the fiber length, preparation of pure, low-loss, stable, stoichiometric glass compounds for appropriate control of viscosity between different glasses involves at the fiber drawing temperature, etc. We may mention that though there is a wide difference in glass transition temperature (T_g) of the two glass systems used in our theoretical modeling, a similar (though less difference in values of T_g's) issue occurs in case of borosilicate glass and silica glass often used in drawing polarization maintaining fibers, which can be solved by appropriate choice of fiber drawing temperature and concentration of the dopants like boron [20, 21]. It is not only T_g but also viscosity as well as thermal expansion coefficients of the constituent glasses that matter while targeting fabrication of a multimaterial optical fiber, and variety of techniques could be employed to fabricate multimaterial fibers [22]. Finally, the important fact that there already exists well-matured fabrication technologies [6, 14–16, 22–25] to draw various chalcogenide MOFs, it should be of interest to invest efforts and money for fabrication of such application specific fibers. Note that, once the design is accepted, fiber fabricators could look for other appropriate glass combinations to solve fabrication issues

#186548 - $15.00 USD Received 6 Mar 2013; revised 20 Mar 2013; accepted 21 Mar 2013; published 10 Apr 2013

using our design as the initial design platform and if necessary fine tune the design parameters. It is worthwhile to mention that, fabrication tolerance for pitch (Λ) and diameter of hole (d) with respect to their average value can be achieved within 2 to 4% [25], which is below the tolerance limit of our designed fiber parameters for stable output as dispersion profiles remains nearly constant except the position of λ_{ZD}. In that case tunable pump (2.71 – 2.88 μm) [2] is needed to maintain the desirable GVD parameters at pump wavelength. Thus scope remains to improve this factor further.

Acknowledgments

This work relates to Department of the Navy (USA) Grant N62909-10-1-7141 issued by Office of Naval Research Global. The United States Government has royalty-free license throughout the world in all copyrightable material contained herein. Some salient features of these results were recently reported by us at the international conference Photonics 2012 held at IIT Madras, Chennai, India. Thanks are due to Ranjan Sen of CGCRI (Kolkata, India) for educating us on the importance and choice of fiber drawing temperature to take into account the interplay of factors like viscosity, dopants concentrations, and mismatch in glass transition temperatures of the glasses involved in drawing an optical fiber. A.B. gratefully acknowledges support provided by CSIR (India) in the form of a Senior Research Fellowship award.

#186548 - $15.00 USD Received 6 Mar 2013; revised 20 Mar 2013; accepted 21 Mar 2013; published 10 Apr 2013